

An Adaptable Low Dimensional Image Generation Model for Eliminating Illumination Influence

[Takashi Toriu, Hiroshi Kamada and Thi Thi Zin]

Abstract— In general, the color of the image taken by a camera changes when the illumination condition changes. However, human being can perceive almost the true color independent of the illumination (color constancy). The low dimensional image generation model has been discussed as a framework for eliminating illumination influence. It defines how the image color is determined from the illumination color, the object color and the camera spectral sensitivity. Traditionally, the low dimensional image generation model has been identified by setting object color basis functions, illumination color basis functions and the camera spectral sensitivity. In this paper, we propose a method for generating the image generation model by training without specifying any basis functions or camera spectral sensitivity. In that purpose, we prepare some sample images including various colors. Using these data, the image generation model is optimized. The experimental results are shown to confirm the effectiveness of the proposed model. (Abstract)

Keywords— Color constancy, low dimensional image generation model, object color, illumination color. (key words)

I. Introduction

Color recognition is one of important functions in computer vision. However, color recognition often fails when illumination condition changes. On the other hand, human being can perceive almost the true color even if the illumination color changes drastically. This ability of eliminating illumination influence is called “color constancy” [1]. To realize this ability on computer vision, a lot of methods have been proposed [2-6].

The papers [2-4] propose methods to eliminate the influences of the illuminant based on so called Gray-world assumption. In these methods, it is assumed that the average of the colors of the objects in the scenes are gray. Some papers propose methods to estimate the illuminant by assuming that the color of objects surface with highest luminance indicates illuminant color [2, 8]. This assumption means that white surface is brightest in white illumination, and this assumption often called Bright-is-white assumption or max-RGB assumption.

Takashi Toriu
Center for Research and Development of Higher Education, Osaka City
University
Japan
toriu@rdhe.osaka-cu.ac.jp

Hiroshi Kamada
Graduate School of Engineering, Kanazawa Institute of Technology
Japan
kamada@neptune.kanazawa-it.ac.jp

Thi Thi Zin
Faculty of Engineering, University of Miyazaki

Japan
thithi@cc.miyazaki-u.ac.jp

Higher order statistics such as correlation between the brightness and the colors is also used to estimate the illuminant color [9-11]. For example, when the illuminant of the scene is reddish, the red colored part of the object in the scene will be brighter than the other part, and the correlation between the brightness and the color red is strong. When the correlation between the brightness and the color red is strong, the illuminant is estimated as red.

As a general framework for eliminating illumination influence, the low dimensional image generation model has been investigated [5-7, 12, 13]. In the low dimensional image generation model, each of the object color and the illumination color is expressed as a linear combination of a few spectral basis functions. Thus, each of the object color and the illumination color can be specified by a few parameters corresponding to weights for the basis functions. As a result, the color of the image can be expressed as a bi-linear function of the illumination color parameter and the object color parameter. The merit of this model is that the problem becomes rather simple because the number of parameters is kept small.

Traditionally, this image generation model has been identified by setting object color basis functions, illumination color basis functions and the camera spectral sensitivity. It is not clear what basis function are optimal. Especially, the camera spectral sensitivity depends on the camera. We should examine the camera spectral sensitivity with respect to each camera.

In this paper, we propose a method to construct an adaptable low dimensional image generation model. In this method, we prepare some appropriate training samples. An example of the sample images is shown in figure 1. The sample images are obtained by taking a photo of a color checker under various illumination conditions. Using these data, the low dimensional image generation model is optimized without assuming basis functions on the object color, the illumination color and the camera spectral sensitivity. In other words, the image generation model is adaptably optimized against the camera and the photographing environment. It is expected that this method would be utilized



as an application for color balance adapted to each particular camera.

Figure 1. An example of test images.

This paper is organized as follows. In the next section, we introduce the image generation model and propose a method for training the image generation model. In the section III, we discuss on the method for elimination influence of illumination color. In the section IV, we confirm the effectiveness of the proposed method by computer simulation. And finally, we conclude in the section V.

II. Image Generation Model

A. Model kernel

Let $I^k(x, y)(k = 1, 2, 3)$ be the pixel values at the point (x, y) on the image plane, where subscript k represents the color component red, green or blue. Let $E(x, y; \lambda)$ be the spectral distribution of the illuminant power, $S(x, y; \lambda)$ be the reflectance of objects surface, and $R^k(\lambda)$ be the spectral sensitivities of the camera. The parameter λ represents wave length of light. Then the following equation holds.

$$I^k(x, y) = \int E(x, y; \lambda) S(x, y; \lambda) R^k(\lambda) d\lambda \quad (1)$$

This equation expresses the image generation model, which indicates how the image is generated. In the low dimensional linear model [6], $E(x, y; \lambda)$ and $S(x, y; \lambda)$ are represented as

$$E(x, y; \lambda) = \sum_{i=1}^3 \eta_i(x, y) E_i(\lambda) \quad (2)$$

and

$$S(x, y; \lambda) = \sum_{j=1}^3 \sigma_j(x, y) S_j(\lambda) \quad (3)$$

respectively. $E_1(\lambda)$, $E_2(\lambda)$ and $E_3(\lambda)$ are the basis functions for $E(x, y; \lambda)$, and $S_1(\lambda)$, $S_2(\lambda)$ and $S_3(\lambda)$ are the basis functions for $S(x, y; \lambda)$. The color of the illumination is represented by $\eta_1(x, y)$, $\eta_2(x, y)$ and $\eta_3(x, y)$, and the color of the object is represented by $S_1(\lambda)$, $S_2(\lambda)$ and $S_3(\lambda)$.

For simplicity, we assume that illumination in parallel. Then, $E(x, y; \lambda)$ is constant and we get

$$E(\lambda) = \sum_{i=1}^3 \eta_i E_i(\lambda) \quad (4)$$

Substituting (3) and (4) into (1), we obtain

$$I^k(x, y) = \sum_{i=1, j=1}^3 \eta_i \sigma_j(x, y) \int E_i(\lambda) S_j(\lambda) R^k(\lambda) d\lambda \quad (5)$$

Equation (5) can be expressed as

$$I^k(x, y) = \sum_{i=1, j=1}^3 \eta_i M^k_{ij} \sigma_j(x, y), \quad (6)$$

where M^k_{ij} is defined as

$$M^k_{ij} = \int E_i(\lambda) S_j(\lambda) R^k(\lambda) d\lambda. \quad (7)$$

We call it the model kernel.

Once the model kernel is obtained, the image color is determined from the object color $\sigma_i(x, y)(i = 1, 2, 3)$ and the illumination color $\eta_i(i = 1, 2, 3)$ according to (6). We are not able to observe $\sigma_i(x, y)$ and η_i directly. However, we can regard $\sigma_i(x, y)$ to be the image when the illumination is white as shown in the Appendix I. Similarly, we can regard η_i to be the image when the object is white. The equation (6) is the low dimensional image generation model.

In conventional low dimensional linear model, basis functions $E_i(\lambda)(i = 1, 2, 3)$, $S_j(\lambda)(j = 1, 2, 3)$ and $R^k(\lambda)(k = 1, 2, 3)$ are assumed to be known, and the model kernel is obtained by (7). Alternatively, in the next sub-section, we propose a method for obtaining the model kernel by training using some sample data.

B. Training the model kernel

We prepare sample images for training the model kernel, in which the white part is included. An example is shown in Figure 1. This image was the image of a color checker under white illumination. The bottom left part is white. We take photos under variety of illuminations including white illumination. The image color under white illumination can be regarded as the object color $\sigma_i(x, y)(i = 1, 2, 3)$ in the image generation equation (6) as is discussed at the end of the last sub-section. When the test image includes T colored regions, we obtain T object colors $\sigma^s_i(x, y)(i = 1, 2, 3; s = 1, 2, \dots, T)$. Also, the image color at the white part under un-known illumination can be regarded as the illumination color $\eta_i(i = 1, 2, 3)$. When images are taken under F kinds illumination conditions, we get F illumination colors $\eta^f_i(i = 1, 2, 3; f = 1, 2, \dots, F)$. Let $I^{k, f, t}(k = 1, 2, 3)$ be the image color corresponding to the illumination color $\eta^f_i(i = 1, 2, 3)$ and the object color $\sigma^t_i(i = 1, 2, 3)$. Then, the next relation holds.

$$I^{k, f, t} = \sum_{i=1, j=1}^3 \eta^f_i M^k_{ij} \sigma^t_j. \quad (8)$$

In this equation, $I^{k,f,t}(k=1,2,3)$, $\eta^f_i(i=1,2,3)$ and $\sigma^t_i(i=1,2,3)$ are known. In order to obtain the model kernel M^{k}_{ij} we define the evaluation function as

$$J = \sum_{f,t,k} \left(I^{k,f,t} - \sum_{i=1,j=1}^3 \eta^f_i M^{k}_{ij} \sigma^t_j \right)^2. \quad (9)$$

The model kernel M^{k}_{ij} is obtained by minimizing the evaluation function (9). To get the solution, we differentiate (9) by M^{k}_{ij} , and set it to be 0.

$$\frac{\partial J}{\partial M^{k}_{ij}} = -2 \sum_{f,t} \left(I^{k,f,t} - \sum_{i=1,j=1}^3 \eta^f_i M^{k}_{ij} \sigma^t_j \right) \eta^f_i \sigma^t_j = 0 \quad (10)$$

From this, we get

$$\sum_{f,t} \eta^f_i I^{k,f,t} \sigma^t_j = \sum_{i',j'}^3 \left(\sum_f \eta^f_i \eta^f_{i'} \right) M^{k}_{i'j'} \left(\sum_t \sigma^t_j \sigma^t_{j'} \right). \quad (11)$$

The model kernel M^{k}_{ij} which minimizes (9) is obtained by solving (11) as a simultaneous linear equation. More specifically, we define 3 x 3 matrices Q^k , Φ and T as

$$\begin{aligned} Q^k_{ij} &= \sum_{f,t} \eta^f_i I^{k,f,t} \sigma^t_j, \\ \Phi_{i'j'} &= \sum_f \eta^f_i \eta^f_{i'}, \\ T_{j'j} &= \sum_t \sigma^t_j \sigma^t_{j'}. \end{aligned} \quad (12)$$

Then, (11) is expressed as

$$Q^k = \Phi M^k T. \quad (13)$$

From this, the model kernel M is obtained as

$$M^k = \Phi^{-1} Q^k T^{-1} \quad (14)$$

Thus, the model kernel is obtained by training using sample images including various colors taken under various illuminations.

III. Elimination of Illumination Influence

We assume that a region of white part is known. Taking the spatial average of (6) in that region, we obtain

$$\langle I^k \rangle = \sum_{i=1,j=1}^3 \eta_i M^{k}_{ij} \langle \sigma_j \rangle. \quad (15)$$

Since the average of the object $\langle \sigma_j \rangle$ is assumed to be white, $\langle I^k \rangle$ would indicate illumination color. Therefore, η_i is considered to be equal to $\langle I^i \rangle$. Therefore, (6) becomes

$$I^k(x, y) = \sum_{i=1,j=1}^3 \langle I^i \rangle M^{k}_{ij} \sigma_j(x, y). \quad (16)$$

Let 3 x 3 matrix E be

$$E_{kj} = \sum_{i=1}^3 \langle I^i \rangle M^{k}_{ij} \quad (17)$$

Then, (16) becomes

$$I^k(x, y) = \sum_{j=1}^3 E_{kj} \sigma_j(x, y) \quad (18)$$

Solving (18), we obtain

$$\hat{\sigma}_j(x, y) = \sum_{j=1}^3 E^{-1}_{jk} I_k(x, y) \quad (19)$$

$\hat{\sigma}_j(x, y)$ is the estimated object color, which is expected to be the image when the illumination is white. Thus, the problem of color constancy is solved.

In this method, a white region in the image should be known. In the Bright-is-white assumption [2, 8], it is assumed that the brightest region in the image is white. In this case, the illumination color η_i is estimated by averaging the image color in the brightest region. Then, the object color at each pixel of the image is estimated as (19).

In the Gray-world assumption, it is assumed that average of the image color $\langle I^i \rangle$ over the whole image is gray. Then, the illumination color η_i would be proportional to $\langle I^i \rangle$. Then, the object color is estimated as

$$\hat{\sigma}_j(x, y) = C \sum_{j=1}^3 E^{-1}_{jk} I_k(x, y), \quad (20)$$

where C is a proportional constant corresponding to overall brightness.

IV. Experiments

A. Training

We trained the model kernel using the color checker shown in Figure 1. We took photos under thirty-five illuminations. Among them, five images were taken under white illumination. We prepared three colored lumps, red, green and blue. Thirty images were taken under one or two colored lumps.

The color checker has twenty-four colored squares. Based on the colors of twenty-four squares under white illuminations, we obtained $T = 24$ object colors $\sigma^t_j(x, y)$ ($t = 1, 2, \dots, T$). Specifically, first, the average color of a predefined area of each square is detected as a color of each square. Then, the color of each square is averaged over ten images under white illuminations. In this way, T object colors $\sigma^t_j(x, y)$ ($t = 1, 2, \dots, T$) are obtained. These data are used not only for training of the model kernel but also for the ground-truth in the evaluation experiment.

Then, based on the color of the white square located at bottom left, we obtained the illumination color. In that time, the color is averaged over a predefined area in the white square. From the image color of this part under $F = 30$ illuminations, we obtained F illumination colors η^f_i ($f = 1, 2, \dots, F$). Also, by observing image color of T squares under F illuminations, we obtained $T \times F$ image colors $I^{k,f,t}$ ($f = 1, \dots, F, t = 1, \dots, T$). Using these data, we trained the model kernel by minimizing the evaluation function (9).

B. Estimation of the object color

We conducted experiments to estimate the object color by eliminating illumination influence. We set one image among thirty images under colored illuminations as a test image for estimating the object color and we trained the model kernel using the rest $T - 1$ images. After the training, we estimated the object color by the method in the last section, and it is compared with the corresponding $\sigma^t_j(x, y)$.

To confirm effectiveness of the proposed method, we conducted a comparison experiment with a method based on the next two simple image generation models. The image generation equation of Model 1 is expressed as

$$\langle I^k \rangle = \sum_{i=1, j=1}^3 \eta_i M^{k,ij} \langle \sigma_j \rangle. \quad (21)$$

As for Model 2, the image generation equation is

$$I^k(x, y) = \beta_k \eta_k \sigma_k(x, y). \quad (22)$$

Model 1 has one overall proportional constant α . On the other hand, Model 2 has three proportional constant β_1, β_2 and β_3 , each of which is corresponding to color red, green and blue.

In the Model 1, the proportional constant α is obtained by minimizing

$$J = \sum_{f,t,k} \left(I^{k,f,t} - \alpha \eta^f_k \sigma^t_k \right)^2. \quad (23)$$

The solution is

$$\alpha = \frac{\sum_{f,t,k} I^{k,f,t} \eta^f_k \sigma^t_k}{\sum_{f,t,k} \eta^{f,2}_k \sigma^{t,2}_k}. \quad (24)$$

Then, the object color is estimated as

$$\hat{\sigma}_k(x, y) = \frac{1}{\alpha \eta_k} I^k(x, y), \quad (25)$$

instead of (19).

In the Model 2, β_k is obtained by minimizing

$$J = \sum_{f,t,k} \left(I^{k,f,t} - \beta_k \eta^f_k \sigma^t_k \right)^2. \quad (26)$$

The solution is

$$\beta_k = \frac{\sum_{f,t} I^{k,f,t} \eta^f_k \sigma^t_k}{\sum_{f,t} \eta^{f,2}_k \sigma^{t,2}_k}. \quad (27)$$

Then, the object color is estimated as

$$\hat{\sigma}_k(x, y) = \frac{1}{\beta_k \eta_k} I^k(x, y). \quad (28)$$

We evaluated effectiveness of the methods numerically by measuring the root mean square error between the estimated object colors and the image color under white illumination. Let $I^{k,f,t}$ ($f = 1, \dots, F, t = 1, \dots, T$) be the image color of the t -th colored square in the test image which is taken under f -th illumination. We train the model kernel using the rest $T - 1$ images. Then, we estimated the object color. Let $\hat{\sigma}^{k,f,t}$ be the estimated object color. We compare it with the ground-truth $\sigma^t_k(x, y)$, which is the image color of the t -th colored square in the image under white illumination. The error is defined as

$$Err(f) = \sqrt{\frac{1}{T} \sum_{t=1}^{24} \sum_{k=1}^3 \left(\hat{\sigma}^{k,f,t} - \sigma^t_k \right)^2}. \quad (29)$$

We show the scatter diagram for $Err(f)$ s by the proposed model and by Model 1 in Figure 2, and $Err(f)$ s by the

proposed model and by Model 2 in Figure 3. The horizontal axis shows $Err(f)$ s by the proposed model, and the vertical axis shows $Err(f)$ s by Model 1 or Model2. We see that $Err(f)$ s by the proposed model are consistently smaller than those by Model1 or Model2.

Next, we average $Err(f)$ over thirty illumination colors ($f = 1, 2, \dots, F$) as

$$Err = \frac{F}{\sum_{f=1}^F Err(f)}. \quad (30)$$

We show the result in the Table 1. The error is reduced by about 10%. The dynamic range of input images is from 0 to 255.

We conducted an experiment to generate the images which represent the object colors. In the same way as the case mentioned above, one image among thirty images under various colored illuminations is selected one after another as a test image and the others are used for the model kernel training. The image representing the object color is estimated as (19). Examples are shown in Figure. 4. Six images in the left-hand side are input images under colored illumination, and six images in the right-hand side are the images indicating the object color estimated by the proposed method. Influence of the illumination colors are effectively reduced.

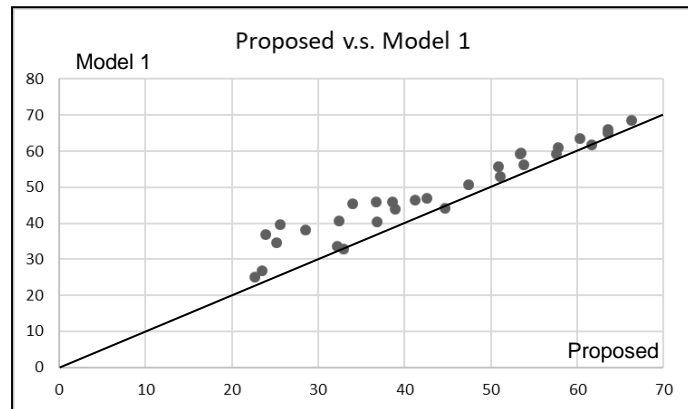


Figure 2. $Err(f)$ s by by the proposed model and Model 1.

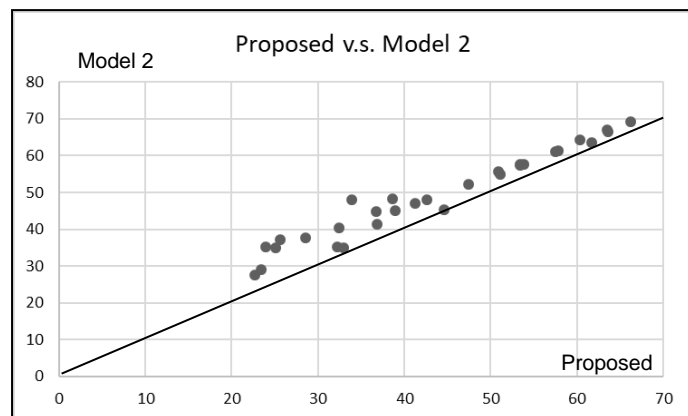


Figure 3. $Err(f)$ s by by the proposed model and Model 1.

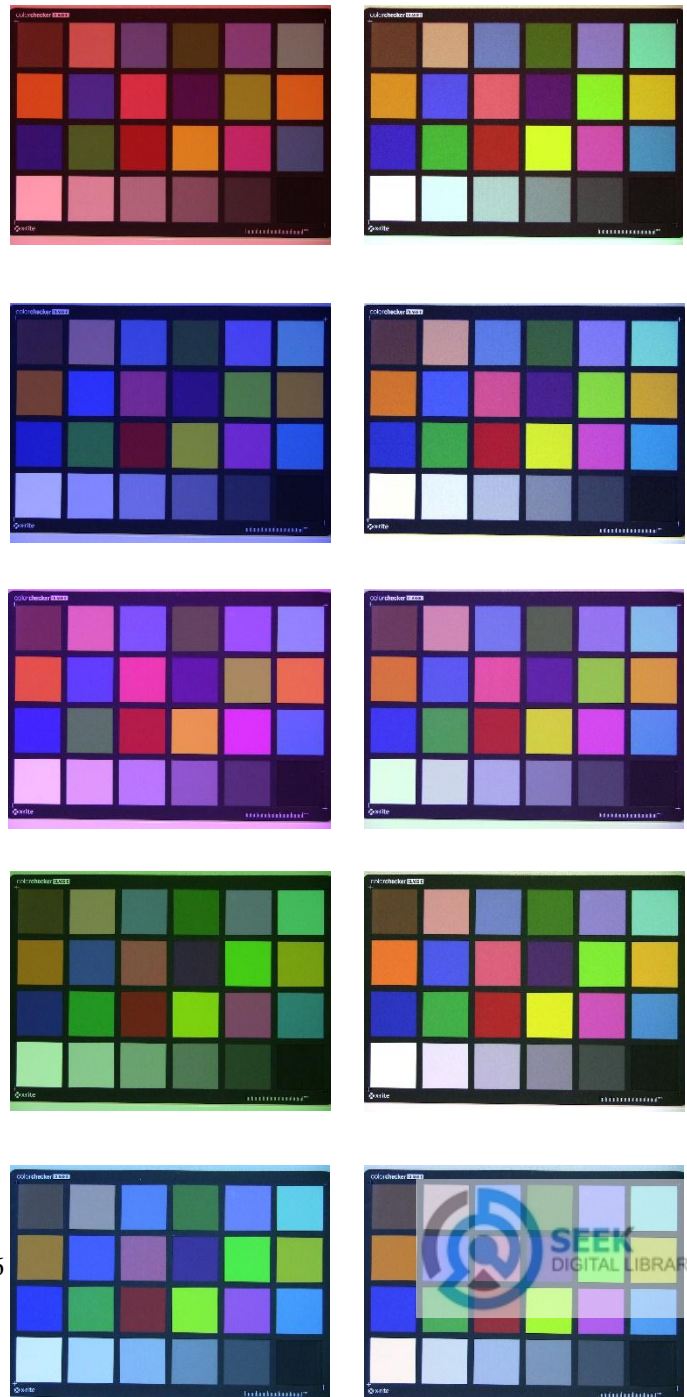
Table 1. Average error.

	Proposed model	Model 1	Model 2
Err	43.4	48.2	48.9

We evaluated the numerical error between the estimated image and the image under white illumination. We compared the proposed model with Model 1 and Model 2. The error is calculated by the following equations. In Model 1 and Model2 the image representing the object color is obtained by (25) or (28).

$$Err(f) = \sqrt{\frac{1}{T} \sum_{x,y,k=1}^3 (\hat{\sigma}_k(x,y) - \sigma_k(x,y))^2}, \quad (31)$$

$$Err = \frac{F}{\sum_{f=1}^F Err(f)}$$



	Proposed model	Model 1	Model 2
<i>Err</i>	56.6	58.7	58.9

v. Conclusion

The low dimensional image generation model is a framework for eliminating illumination influence. In this paper, we proposed the method to obtain an adaptable low dimensional image generation model. The low dimensional image generation model is adaptably optimized using various images of a color checker under variety of illuminations. Some images should be taken under known white illumination, and the region with white color should be detected in advance. On this condition, the image generation model was optimized by minimizing the evaluation function (9). Once the image generation model was obtained, the object color is estimated if a region with white color is detected.

We conducted an experiment to generate the images which represent the object colors. We compared the performance of the proposed image generation model with two naïve and simple image generation models. From this experiment, we confirmed that the proposed model has a competitive advantage over the two naïve and simple image generation models.

It is a future problem to apply this method to different kinds of real images and to confirm effectiveness of this method as color constancy.

Appendix

We assume that $\eta_i (i=1,2,3)$ is 1 when illumination is white and that $\eta_i (i=1,2,3)$ is 0 when illumination is black without loss of generality. In the same way, we assume that $\sigma_i(x,y) (i=1,2,3)$ is 1 when the object is white and that $\sigma_i(x,y) (i=1,2,3)$ is 0 when the object is black. Then, (6) becomes

$$I_o^k(x,y) = \sum_{j=1}^3 \left(\sum_{i=1}^3 M^{kij} \right) \sigma_j(x,y), \quad (A-1)$$

when the illumination is white. From this equation, we see that the object color $(\sigma_1, \sigma_2, \sigma_3)$ and the image color (I_o^1, I_o^2, I_o^3) are connected by a linear transformation. This means that there exist 2 x 2 matrix \tilde{M} such that the next relation holds.

$$\sigma_j(x,y) = \sum_{k=1}^3 \tilde{M}_j^k I_o^k(x,y). \quad (A-2)$$

In the same way, when the object is white, (6) becomes

$$I_e^k = \sum_{i=1}^3 \eta_i \left(\sum_{j=1}^3 M^{kij} \right) \quad (A-3)$$

Figure 4. Examples of estimation of the object color.

We show the scatter diagram for $Err(f)$ by the proposed model and by Model 1 in Figure 5, and $Err(f)$ by the proposed model and by Model 2 in Figure 6. We also show the average error Err in the table 2. We see that the error is effectively reduced in the proposed model.

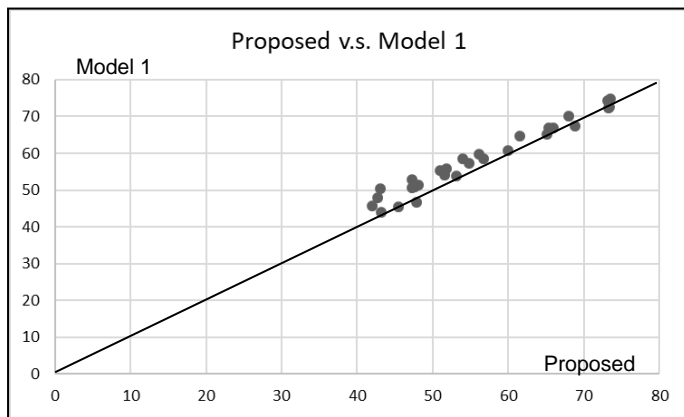


Figure 5. $Err(f)$ by the proposed model and Model 1.

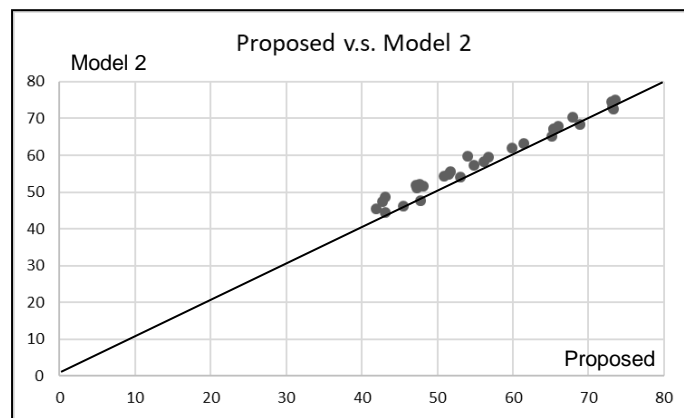


Figure 6. $Err(f)$ by the proposed model and Model 1.

Table 2. Average error.

The vector (η_1, η_2, η_3) and the corresponding vector (I_e^1, I_e^2, I_e^3) are connected by a linear transformation, too. Therefore, there exist 2×2 matrix \hat{M} such that the next relation holds.

$$\eta_i(x, y) = \sum_{k=1}^3 I_e^k(x, y) \hat{M}^k_i \quad (A-4)$$

Substituting (A-2) and (A-4) into (6), we obtain

$$\begin{aligned} I^k(x, y) = & \sum_{i=1, j=1}^3 \left(\sum_{k'=1}^3 I_e^{k'} \hat{M}^{k'}_i \right) M^{k}_{ij} \left(\sum_{k''=1}^3 \tilde{M}_j^{k''} I_o^{k''}(x, y) \right) = \\ & \sum_{k'=1, k''=1}^3 I_e^{k'} \left(\sum_{i=1, j=1}^3 \hat{M}^{k'}_i M^{k}_{ij} \tilde{M}_j^{k''} \right) I_o^{k''}(x, y) = \\ & \sum_{i=1, j=1}^3 I_e^i L^{k}_{ij} I_o^j(x, y), \end{aligned} \quad (A-5)$$

This equation has the same form as (6). In fact, resetting I_e^i by η_i , $I_o^j(x, y)$ by $\sigma_j(x, y)$ and L^{k}_{ij} by M^{k}_{ij} , we obtain the same equation as (6). Thus, we can regard $\sigma_i(x, y)$ to be $I_o^i(x, y)$, the image when the illumination is white and η_i to be I_e^i , the image when the object is white.

Acknowledgment

This work was supported by JSPS KAKENHI Grant Number 15K01041.

References

- [1] Foster.D.H, "Color constancy ", Vision Research, **51**, 674-700, (2011).
- [2] K. Barnard, V. Cardei, B. Funt "A comparison of computational color constancy algorithms. Part I: Methodology and experiments with synthesized data", IEEE Trans, IP, **11**, No.9, 972 -984, (2002).
- [3] H. Kawamura, K. Fukushima, N. Sonehara, "Mathematical conditions for estimating illumination color based on gray world assumption", Proceedings of the Society Conference of IEICE, 167, (1995).
- [4] F. Ciurea, B. Funt, "A Large Image Database for Color Constancy Research", IS&T/SID Eleventh Color Imaging Conference, (2003).
- [5] Mi. D'Zmura and G. Iverson, "Color constancy. I. Basic theory of two-stage linear recovery of spectral descriptions for lights and surfaces", Opt. Soc. Am. A, vol.10, No.10, 2148-2165, (1993).

- [6] T. Teranishi, T. Toriu, "A Method of Estimating Non-parallel Illumination Based on Extended Gray-world Assumption", IJCSN International Journal of Computer Science and Network Security, **11**, No.3, 139-146, (2011).
- [7] L. T. Maloney and B. A. Wandel, "Color constancy: a method for recovering surface spectral reflectance," J. Opt. Soc. Am. A, **3**, 4-9, (1994).
- [8] Brill. M, West. G, "Contributions to the theory of invariance of color under the condition of varying illumination", Journal of Mathematical Biology, **11**, 337-350, (1981).
- [9] Golz. J, MacLeod. D. I. A, "Influence of scene statistics on colour constancy" Nature, **415**, 637-640, (2002).
- [10] Golz. J, "The role of chromatic scene statistics in color constancy: Spatial integration", Journal of Vision, **8(13):6**, 1-16, 2008.
- [11] Granzier. J. J. M, Brenner. E, Cornelissen. F. W, Smeets. J. B. J, "Luminancecolor correlation is not used to estimate the color of the illumination", Journal of Vision, **5**, 20-27, (2005).
- [12] Brill, M. H, "A device performing illuminant-invariant assessment of chromatic relations. Journal of Theoretical Biology", **71**, 473-478, (1978).
- [13] Brill. M. H, "Further features of the illuminant-invariant trichromatic photosensor", Journal of Theoretical Biology, **78**, 305-308, (1979). [1] H. L. Premaratne and J. Bigun. A segmentation-free approach to recognise printed Sinhala script using linear symmetry. *Pattern Recognition*, 37(10): 2081-2089, 2004.

About Author (s):



Takashi Toriu received the Dr. Sci. degrees in Physics from Kyoto University, Japan. He is currently specially appointed professor at Osaka City University. His research interests include image processing, computer vision, mechanism of visual attention. He is a member of IEEE, IEICE, ITE and IEEJ.